JOURNAL OF MATERIALS SCIENCE 31 (1996) 4267–4276

Martensitic transformations in Ti–(16–26 at %) Nb alloys

T. AHMED, H. J. RACK
Materials Science and Engineering Program, Department of Mechanical Engineering, Clemson University, Clemson, SC 29634, USA

Martensitic phase transformations in the solution-treated and water-quenched binary Ti–Nb alloys in the range of 16–26 at % Nb, were examined. An ordered, base-centred orthorhombic martensite was observed for alloys containing up to 23.4 at % Nb. The substructure of this martensite was generally composed of twins and stacking faults, the presence of antiphase boundaries observed in the plates indicating that the martensite underwent ordering during quenching. Both order–disorder and M_s temperatures were observed to be affected by total interstitial content, higher contents increasing both temperatures. Increasing the niobium content to above 23.4% resulted in retention of the β phase, this phase containing either athermal ω or "diffuse" ω depending upon niobium and total interstitial concentration. Finally, the microhardness of the Ti–Nb alloys examined was observed to decrease with increase in niobium and decrease in total interstitial content.

1. Introduction

While extensive examinations of phase equilibria in Ti–Nb alloys have shown that the α (h c p) and β (b c c) are the low-temperature stable phases, Fig. 1, quenching of the β phase from elevated temperatures can result in the formation of two metastable martensitic structures, α′ (hexagonal) and α″ (orthorhombic) [2]. α′ is observed in alloys containing less than 7.2 at % Nb whereas alloys containing $>7.2\%$ Nb content transform to an α″ orthorhombic martensite [3]. Transformation of β to α′ involves (i) shearing of atoms in the $[1\,1\,1]_\beta$ direction within the $(1\,1\,2)_\beta$ plane to $(1\,1\,0\,0)_{\alpha'}$, and (ii) shuffling of atoms in every other atomic plane from $(1\,1\,0)_\beta$ to $(0\,0\,0\,1)_{\alpha'}$ [4]. Additional shuffling of atoms in alternate $(1\,1\,0)_\beta$ planes results in a C-centred α″ orthorhombic crystal structure with a *Cmcm* space group [2, 5–9], atoms located at (0, 0, 0) (1/2, 1/2, 0), (0, 1-2*y*, 1/2) and (1/2, 1/2-2*y*, 1/2) positions, the value of *y* being ≈ 0.2 in Ti–Nb alloys [6, 9]. Thus, α″ may be viewed as a transitional phase between the α′ hexagonal structure and the β b c c structure. Indeed altering the values of *b*/*a*, *c*/*a* and *y*, permits all three structures, α′, α″ and β, to be produced. Ultimately, at higher niobium contents, α″ formation is not observed, instead athermal ω (hexagonal) phase or "diffuse" ω is observed in quenched Ti–Nb alloys containing between 14 and 34% Nb [3, 7, 9–12].

A summary of previous studies involving alloys of compositions Ti–17%–35% Nb is given in Table I. This information indicates that, in addition to composition, changes in either cooling rate or total interstitial content can also result in different microstructures. For example, at 21.8% Nb, α″ is the predominant phase observed in a commercially produced alloy upon water quenching from 900 °C [15]. Oil quenching a similar composition with an oxygen content of 513 w.p.p.m. yields β + ω (with traces of α″) [10] while furnace cooling an alloy containing 1500 w.p.p.m. oxygen and nitrogen, and 200 w.p.p.m. hydrogen from 900 °C resulted in β + α″ + ω [17]. Similarly, effects of solution-treatment time and temperature on the quenched microstructure have also been observed.

A major effort was made by Moffat and Larbalestier [3] to clarify these transformations by examining the phase transformations in alloys containing 20%–70% Nb emphasizing careful chemical analysis of alloys and considering the effect of quench rate on microstructure. It was observed that on water quenching from 1000 °C, α″ was present in alloys containing between 20% and 25% Nb, whereas single-phase β and "diffuse" ω were observed in alloys containing higher amounts of niobium. On air cooling, ω precipitates were observed in alloys containing 20%, 25%, 30% and "diffuse" ω in 35% Nb; on furnace cooling, 35% Nb contained ω particles rather than "diffuse" ω. These authors concluded, therefore, that upon quenching of the β phase, formation of the α″ and ω phases is a competitive process occurring within an unstable lattice, faster quench rate favouring α″ formation, slow cooling promoting ω. These observations have been extended in the present work, where martensitic transformations observed in Ti–(16–26 at %) Nb alloys have been studied.

2. Experimental procedure

Ti–Nb binary alloys were prepared from high-purity titanium (O < 240 w.p.p.m., N < 26 w.p.p.m., C = 9.9 w.p.p.m.) and niobium (O < 60 w.p.p.m., N = 29 w.p.p.m., C = 19 w.p.p.m., Si < 50 w.p.p.m.) by arc

0022–2461

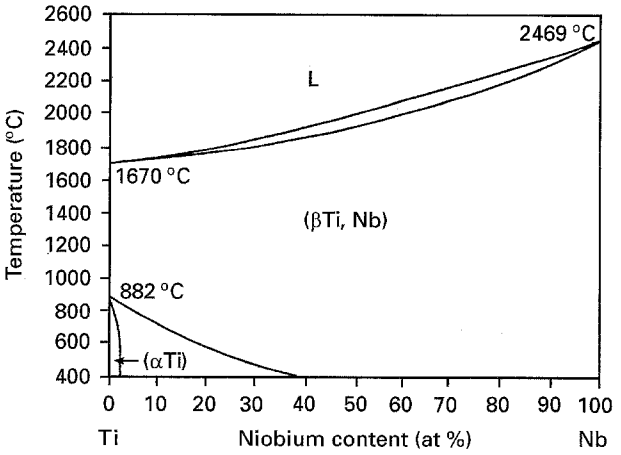

Figure 1 Assessed Ti–Nb diagram by Murray [1].

melting. Before weighing and melting, the constituents were cleaned in alcohol to remove surface contaminants and the high-purity titanium sponge was melted to minimize splattering-associated weight losses during subsequent incorporation with niobium. The molten titanium and pure niobium were weighed with a balance of accuracy of $\pm$ 0.0005 g to make up an alloy of 30 g. Melting was carried out in a high-purity (1 w.p.p.b.) argon atmosphere, water-cooled copper hearth non-consumable tungsten electrode arc furnace. Prior to melting, a titanium getter was melted in the furnace which had been evacuated and flushed three times with purified argon. The alloys were melted at least five times, each time being held in the molten state for 2–3 min, the button being flipped between each melt. After melting the alloys were reweighed, the percentage weight loss being observed to vary between 0.4% and 1.3%.

The buttons were then cleaned with alcohol, wrapped in tantalum foil and encapsulated in quartz tubes together with a small quantity of titanium sponge under a 25 torr (1 torr = 133.322 Pa) partial pressure of high-purity argon. All alloys were homogenized at 800 °C for 168 h and furnace cooled. Samples of the homogenized alloys were utilized for chemical analyses, Table II. Finally, encapsulated homogenized samples of all alloys were solution treated at 1000 °C for 0.5 h and water quenched.

Characterization of the microstructures involved hardness, X-ray diffraction, optical and transmission electron microscopy. The hardness measurements, an average of ten readings, were carried out on a Micromet microhardness instrument using a 200 g load, a standard deviation of $\pm$ 5 VHN being typically observed in the determined hardness.

Room-temperature X-ray diffraction analysis was carried out on a SCINTAG diffractometer utilizing

TABLE I Summary of the results obtained in the previous studies involving alloys containing niobium contents between 17 and 35 at %

Reference	Compos. (at % Nb)	Interstitial Content[a] (w.p.p.m)	Temp. (°C)/ time (h)	Cooling rate (°C s^{-1})	Phases observed
[13]	17.4–21	NR[b,c]	700/335	WQ[b]	α, β
[2,6,8]	17.4	O,N:706[d]	NR, but	0.2	α, β
	17.4	O,N:706[d]	from β	940	α″
	17.4	O,N:706[d]	phase	19000	β
	20.0	O,N:706[d]		WQ	α″
	24.8	O,N:706[d]		WQ	β
[14]	21.8	O,N,C:100	800/3	VC[b]	β
[15]	21.8	NR[e]	900/NR	WQ	α″
[16]	21.8	O:350[d]	1000/2	WQ	β
[10][f]	18	O:1210	900/5	OQ[b]	α″, β_o^g, β_e^h
	18	O:1210	1000/5	OQ	β, ω, $\alpha''^{i,j}_{tr}$
	21.8	O:513	800/3	OQ	α″, β[k]
	21.8	O:513	900/5	OQ	β, ω, α''^{j}_{tr}
	21.8	O:513	1000/5	OQ	β, ω[k]
	25.0	O:960	900/5	OQ	β, ω
[17]	21.8	O,N:1500 H:200	900/2	FC[b]	β, α″, ω
[11]	21.8	NR	1000/.25	Liq. N_2Q	β, ω
[3]	20	O,N,C:1090[l]	1000/8	WQ	α″, β
	25	O,N,C:1026	1000/8	WQ	α″, β
	30	O,N,C:1229	1000/8	WQ	β, diff ω[m]
	35	O,N,C:880	1000/8	WQ	β, diff ω[m]

[a] Interstitial contents prior to heat treatment.
[b] NR, not reported; WQ, water quench; OQ, oil quench; VC, vacuum cool; FC, furnace cool,
[c] Used titanium iodide.
[d] Contents of the starting material.
[e] Used commercially produced alloy.
[f] All alloys in this study were initially homogenized at 1000 °C for 24 h in vacuum.
[g] β_o, β of original composition.
[h] β_e, β enriched in Nb.
[i] tr, trace.
[j] Also contains TiC.
[k] Also contains trace of TiC.
[l] Interstitial contents determined after heat treatments.
[m] Diff ω, "diffuse" ω streakings and maximas in the selected-area diffraction patterns.

TABLE II Niobium, oxygen, nitrogen and carbon contents of the homogenized alloys

Alloy	Nominal Nb content (at %)	Actual Nb content (at %)	O (w.p.p.m.)	N (w.p.p.m.)	C (w.p.p.m.)	Total interstitials[a] (w.p.p.m.)
Nb17	16.7	17.6	600	80	150	830
Nb18	18.8	18.2	370	80	70	550
Nb19H	19.5	18.7	600	140	160	900
Nb19L	19.5	19.4	400	60	40	500
Nb20	20.2	19.6	370	30	40	440
Nb21L	21.0	21.4	500	60	60	620
Nb21H	21.8	21.4	600	480	100	1180
Nb22H	22.5	21.7	600	320	100	1020
Nb22L	22.5	21.9	370	30	50	450
Nb23	23.2	23.4	700	350	120	1170
Nb24	24.0	24.1	500	30	130	660
Nb25	24.8	24.9	600	310	170	1080
Nb26	25.6	25.6	600	210	130	940

[a] O + N + C.

CuK_α radiation at 40 kV and 30 mA, the scanning rate being $5°2\theta\ min^{-1}$ from $2\theta = 20° - 80°$. Following data collection, lattice parameters determination and peak indexing followed a least square method iterative computer program [18], the average errors in the values of lattice parameters *a*, *b* and *c* being estimated to be ± 0.0007 nm, ± 0.003 nm and ± 0.003 nm, respectively.

Finally, the solution-treated microstructures were observed by optical and transmission electron microscopy. Samples for optical microscopy were prepared by rough and fine polishing followed by etching with 8 vol % HF, 15 vol % HNO_3 and 77% H_2O, while transmission electron microscopy samples were mechanically wafered, ground to 0.15 mm thickness and electropolished in a solution of 5 vol % H_2SO_4, 2 vol % HF and 93 vol % methanol under the voltage and temperature conditions of 15–20 V and $-40\,°C$. Duplicates of selected samples were also prepared by ion milling, utilizing a current of 0.5 mA and voltage 4–5 kV, the latter specimen preparation technique being used to eliminate any ambiguity that might rise from electropolishing, *e.g.* thinning transformations. A Hitachi 600 AB electron microscope (operated at 100 kV) was used for these observations.

3. Results

3.1. Optical microstructures

After solution treatment, the alloys Nb17–Nb23 (Nb content 16.7%–23.2%) were two-phase, martensite + β, with the volume fraction of martensite decreasing with increasing niobium content. In contrast, alloys Nb24, Nb25 and Nb26 (Nb content 24.0%–25.6%) were 100% retained β, Fig. 2. Alloys Nb17 and Nb21H contained long and relatively thick primary martensite plates with a large number of fine secondary plates. Other large plates without distinct boundaries were also observed in these alloys, Fig. 2a and b. The former long primary plates were absent in alloys Nb22L and Nb23, fine martensitic plates with reduced volume fraction being observed, Fig. 2c and d. Alloy Nb23 was also observed to contain large plates without distinct boundaries as seen in alloy Nb17 and Nb21H, Fig. 2d. Finally, although alloys Nb21H and Nb22L had similar compositions, 21.4% and 21.9% Nb, respectively, the volume fraction of martensite was higher in the former alloy, presumably due to the higher total interstitial content of this alloy (Table II).

3.2. Hardness response

Fig. 3 shows the hardness response of the solution-treated and quenched Ti–Nb alloys as a function of niobium content, total interstitial contents of each alloy also being given. The hardness results lay within a broad band decreasing, at constant interstitial content, with increasing niobium content and increasing, at constant niobium content, with increasing total interstitial content. The latter observation is in accordance with the observed effect of increase in interstitial on the hardness in other titanium alloys. The upper limit of the band corresponds to the interstitial content between 830 and 1130 w.p.p.m., whereas the lower limit is for the range 440–660 w.p.p.m.

3.3. X-ray diffraction

Room-temperature X-ray diffraction indicated that the martensite phase observed in the alloys investigated had an orthorhombic crystal structure, Fig. 4a and b. Lattice parameter measurements of the orthorhombic structure, Fig. 5, indicated that *a* increased with increasing niobium content, while the *b*/*a* and *c*/*a* ratios decreased with increasing niobium, in accordance with trends previously observed [3].

3.4. Transmission electron microscopy

Transmission electron microscopy of the solution-treated alloys confirmed that orthorhombic martensite was formed on quenching alloys between 16% and 23.4% Nb and β + ω in alloys between 24% and 26% Nb. These observations also showed that α″ produced had a strained and highly faulted substructure, Fig. 6a, with a few plates internally twinned,

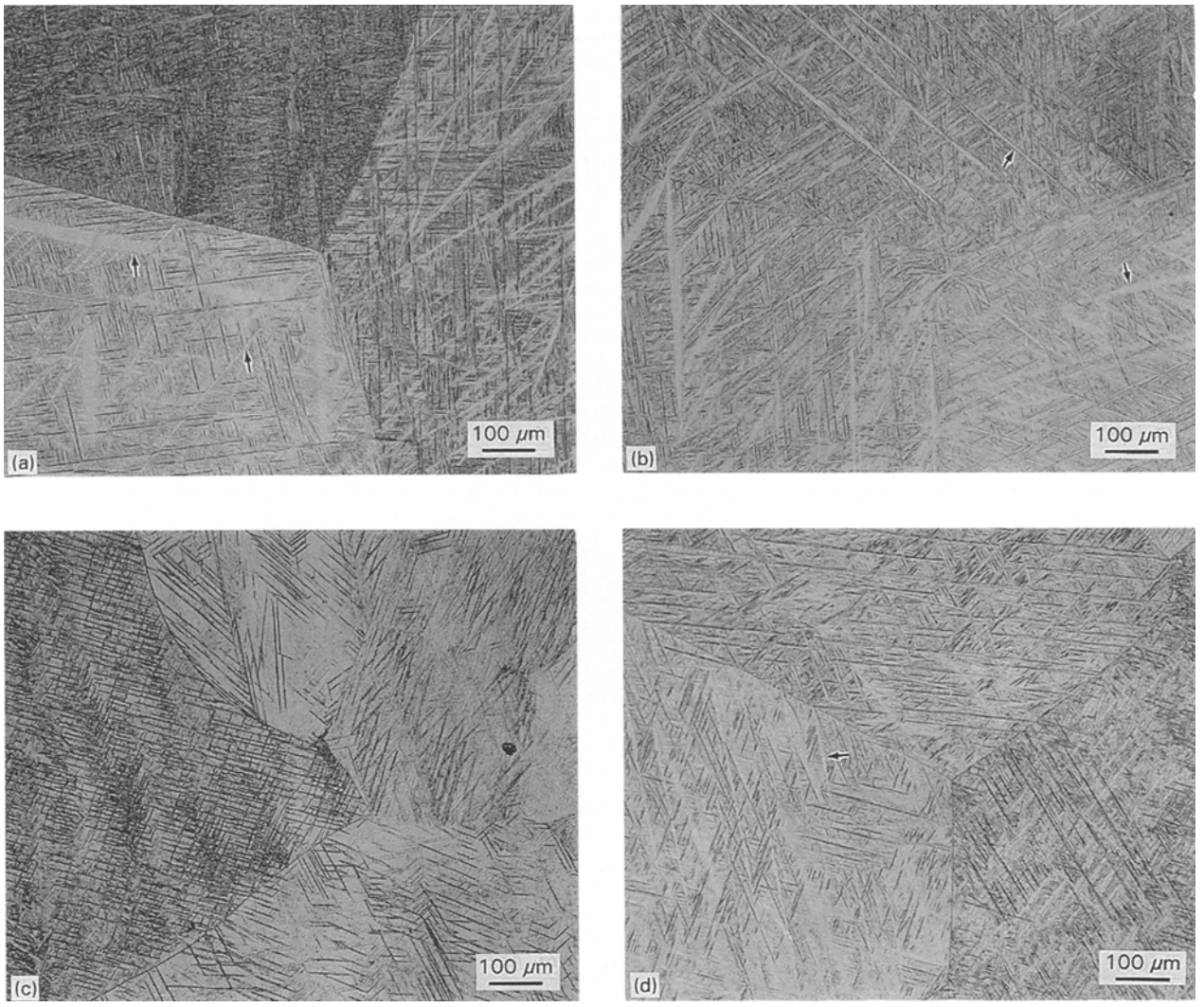

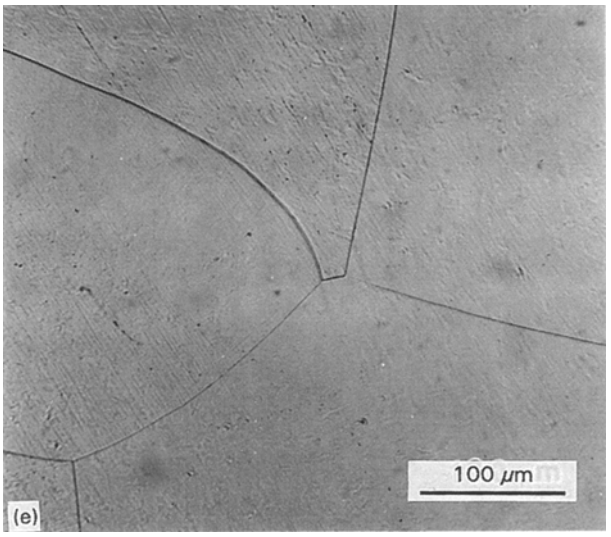

Figure 2 Optical micrographs of solution-treated and quenched alloys: (a) Nb17, (b) Nb21H, (c) Nb22L, (d) Nb23, (e) Nb26. The primary martensitic plates having distinct and non-distinct boundaries, are indicated by arrows.

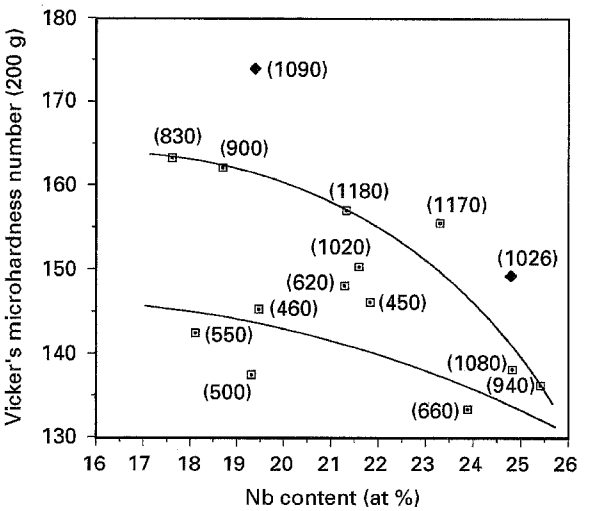

Figure 3 Variations in hardness values with niobium contents. The total interstitial contents are given in parentheses. (◆) The hardness values of alloys studied by Moffat [20]. (⊡) Present work.

Fig. 6b, the twin plane in these instances being $\{1\,1\,1\}\alpha''$. Fig. 6c shows a complex selected-area diffraction pattern (SADP) of the [0 0 1] β zone with two variants of the [1 0 0] α″ zone. This SADP confirmed the following orientation relationship: $[0\,0\,1]\beta // 3°[1\,0\,0]\alpha''_1$, $(1\,1\,0)\beta // (0\,0\,1)\alpha''_1$ and $[0\,0\,1]\beta // 3°[1\,0\,0]\alpha''_2$, $(1\,1\,0)\beta // (0\,0\,1)\alpha''_2$, as previously reported [7, 9]. A few plates also contained ribbon-like stacking faults lying on more than one crystallographic plane, Fig. 7a, similar to those observed in other titanium–transition element orthorhombic martensites [19]. The large primary plates were observed to have

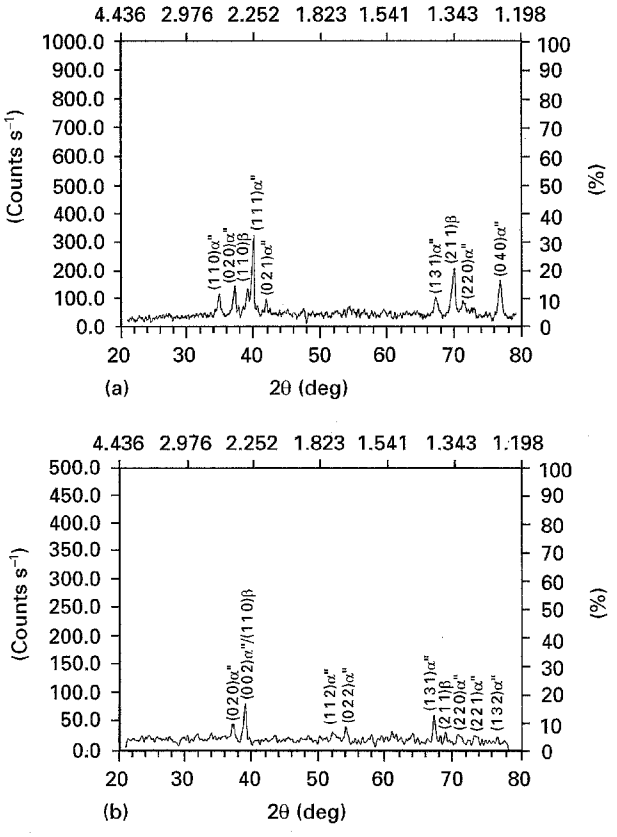

Figure 4 Room-temperature X-ray diffraction patterns of solution-treated and quenched alloys: (a) Nb17, (b) Nb21H.

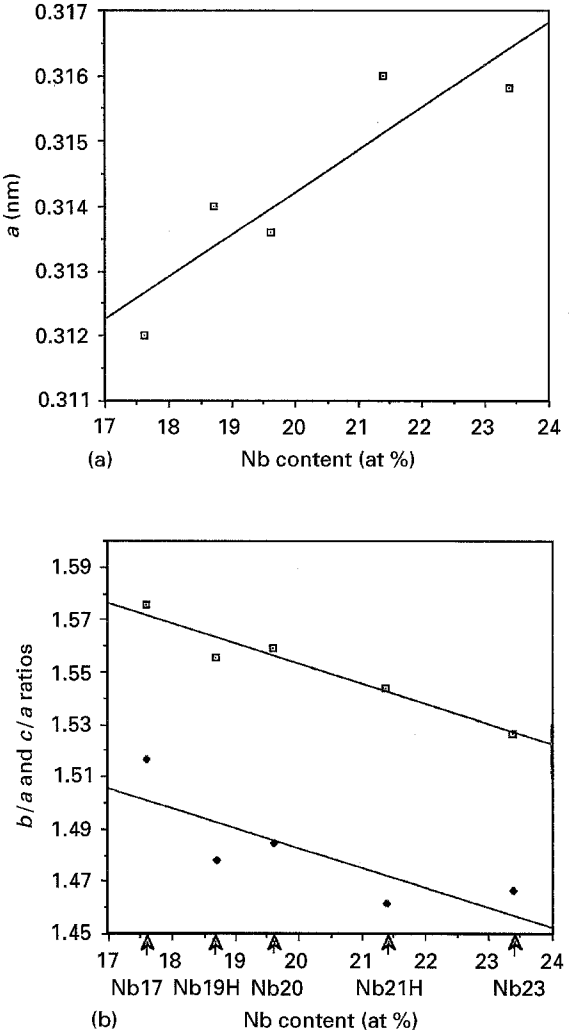

Figure 5 The variation of lattice parameters of orthorhombic martensite with niobium content: (a) a parameter, (b) (□) b/a and (◆) c/a ratios.

antiphase boundaries (APBs), Fig. 7b, as were a number of smaller plates, *e.g.* lower left portion of Fig. 6a, suggesting that the α″ martensite ordered during quenching. Other than Nb22L, APBs containing plates were observed in all alloys. Further, SADPs taken from plates containing APBs and stacking faults indicated extra reflections of the (0 0 1) type, Figs 6c and 7c. This is not an allowed reflection for the previously proposed orthorhombic unit cell of α″ martensite [6, 9] as shown in Fig. 8a. However, a base-centred unit cell, Fig. 8b, with titanium atoms at 0, 0, 0 and niobium and extra titanium atoms at 1/2,1/2,0 positions, is consistent with these reflections.

A small volume fraction of retained β phase containing athermal ω particles was also observed lying between the martensite plates in alloys Nb21H and Nb23. Transmission electron microscopy of Nb22L indicated the presence of a similar faulted substructure within the martensite platelets as in other alloys but with a higher volume fraction of the retained β phase, Fig. 9a, with very fine particles of athermal ω phase have being observed and confirmed by SADPs, Fig. 9b and c. These observations were also confirmed in Nb17, Nb21H and Nb22L prepared by ion milling, Fig. 10 shows the presence of APBs in α″ martensitic plates in a Nb17 ion-milled sample.

Finally, study of Nb24 and Nb26 confirms the presence of retained β, SADPs of the former showing ω reflections, whereas streaking, indicative of "diffuse" ω phase, was observed in the later alloy, Fig. 11a and b, respectively.

4. Discussion

4.1. Compositional influence on microhardness

The change in hardness with increasing niobium content (within the composition range studied) follows a trend similar to that observed in previous studies [5, 20], the initial decrease being ascribed to the decrease in volume fraction of α″, the larger decrease at higher niobium contents being related to the reduction in the volume fraction of the athermal ω phase with increasing niobium content. However, Fig. 3 shows that increasing the interstitial contents actually has a more pronounced effect on hardness values than does the variation in niobium content. This result is consistent with the observed solid-solution hardening element role of interstitial elements oxygen, nitrogen and carbon, and is confirmed by the hardness values of Moffat [20], Fig. 3, where alloys of compositions of 20% and 25% Nb have higher hardness values due to the higher total interstitial contents of their alloys.

4.2. Phase equilibria

Table III summarizes the phases observed in the solution-treated alloys. Water quenching from the β-phase

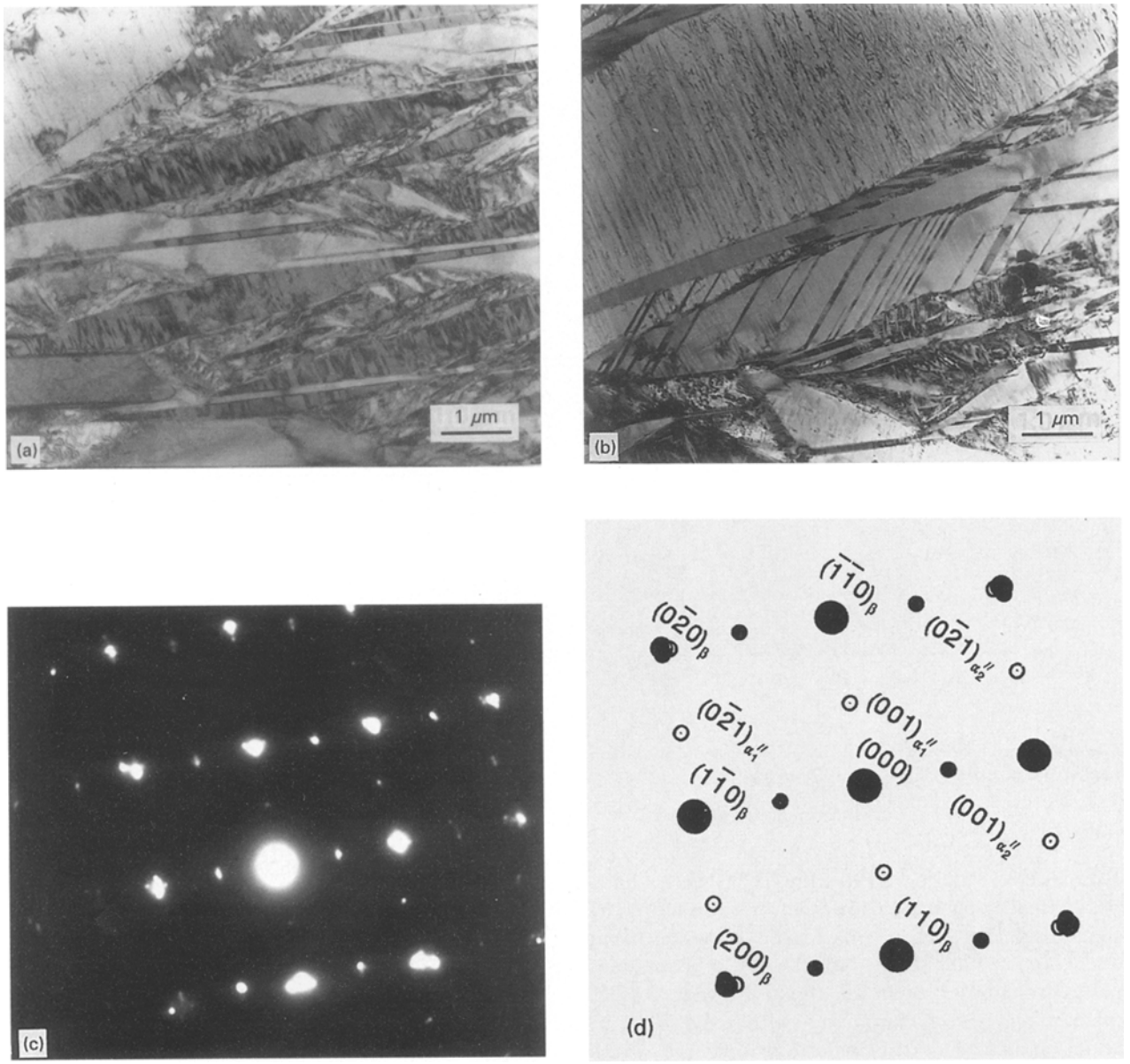

Figure 6 (a) Bright-field-TEM image of alloy Nb17 showing α″ martensite plates. (b) Bright-field-TEM of alloy niobium showing twins in α″ martensite plates. (c) SADP taken from alloy Nb17. Zone axis of the matrix $[0\,0\,1]_\beta$ with two variants of $[0\,0\,1]_{\alpha''}$ zones. (d) Index of the SADP shown in (c).

field produced several different microstructural variants depending upon niobium and total interstitial content. Lower niobium contents exhibited a predominant α″ microstructure with a small amount of retained β, the amount of α″ decreasing and β increasing with an increase in niobium content or decrease in total interstitial contents. At a niobium content $> 23.4\%$, orthorhombic α″ was no longer observed, the microstructure being β + ω. In Nb21H, Nb22L, Nb23 and Nb24, the ω phase was observed in the retained β matrix, whereas "diffuse" ω was observed in the alloy Nb26. Comparison of Nb20 and Nb25 with Moffat and Larbalestiers' alloys [3] shows agreement at the lower niobium content; however, at 25% Nb, these authors reported the presence of α″ along with the ω phase within the β matrix (Table I), this disagreement being ascribed to the higher oxygen content (difference of ≈200 w.p.p.m.) of the alloy studied in the previous work. In contrast, Mendiratta *et al.*'s [16] examination of 21.8% Nb showed a single-phase β microstructure. Unfortunately, chemical analysis was not reported in the latter study after melting.

4.3. Martensite structure and morphology

The α″ martensite observed was morphologically similar to that reported previously [5, 6] having an acicular morphology. Moreover, two type of plates were observed: (i) long, relatively thicker, primary plates with or without distinct boundaries (the appearance of the distinct boundaries being dependent on the orientation of the plate); and (ii) fine, secondary plates. While the size and volume fraction of the large plates decreased with increasing niobium content, the higher interstitial content alloys, at a fixed niobium concentration, had an increased volume fraction of martensite plates, especially the long primary plates. However, there appeared to be no effect of variation in the total interstitial content on the morphology of the martensite, in agreement with Ti–Mo alloys [19].

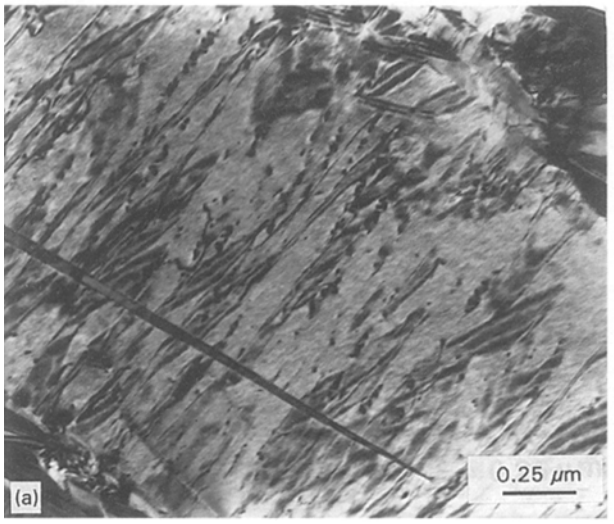

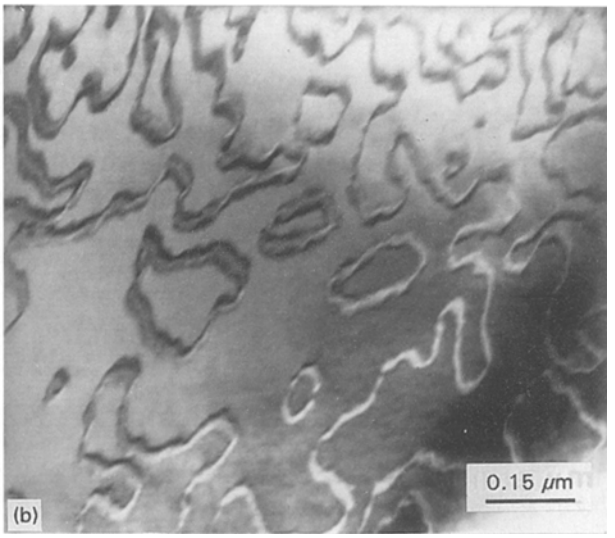

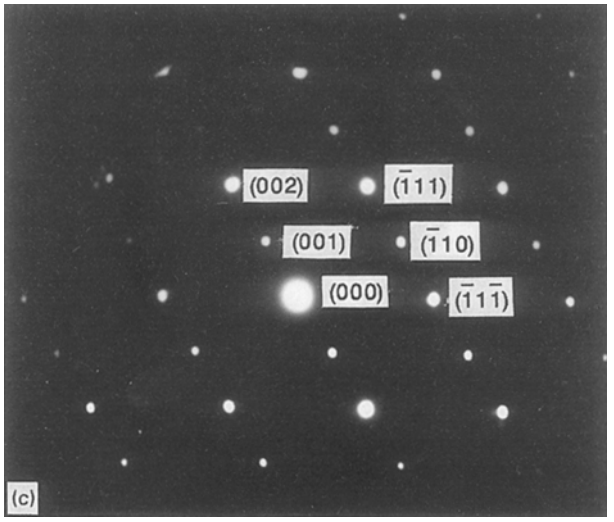

Figure 7 (a) Ribbon-like stacking faults within martensite plates of alloy Nb17. (b) APB network in a large martensite plate in alloy Nb21H. (c) SADP taken from the large plate shown in (b), zone axis $[1\,1\,0]_{\alpha''}$.

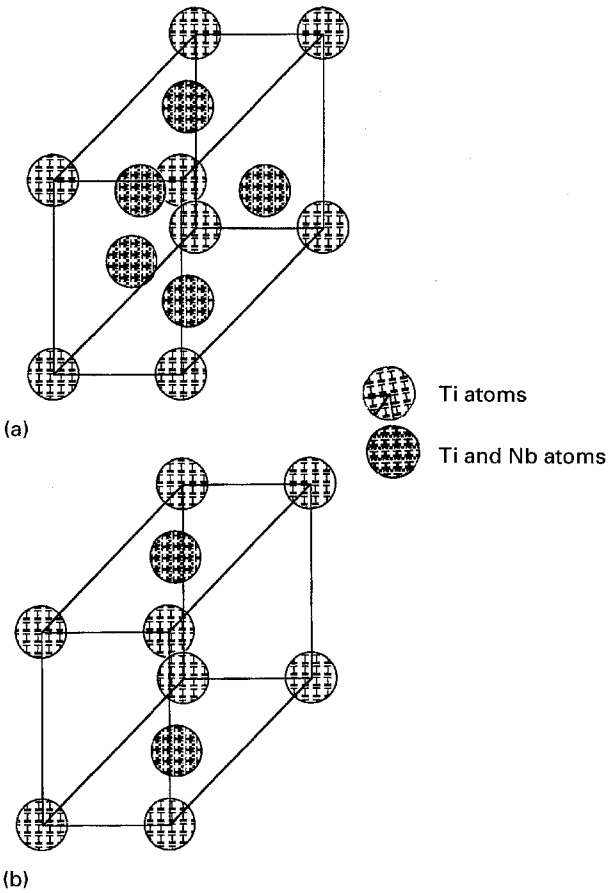

Figure 8 Unit cells of orthorhombic martensite: (a) disordered C-centred, (b) ordered base-centred.

The martensitic substructure was composed of stacking faults and twins. The presence of $\{1\,1\,1\}\alpha''$ twins suggests a preference for twinning over slip in the lower symmetry α'' structure. Similar preference for twinning over slip was observed in deformed single- and polycrystalline Ti–(19–38 at %) V alloys [21, 22]. Further, in alloys containing a higher total interstitial content or lower niobium content, the presence of APBs indicated that ordering of the α'' martensite took place during quenching, the order–disorder temperature lying below the M_s temperature. SADPs also gave reflections of the $(0\,0\,1)\,\alpha''$ and $(0\,0\,3)\,\alpha''$ type, which are not allowed for C-centred orthorhombic unit cell [6], an ordered unit cell based on base-centred orthorhombic, Fig. 9b, being preferred. A similar ordered martensite has also been observed in another quenched titanium-based alloy having a composition of Ti–14.2 V–6.9 Al (at %) [23]. However, in the latter study, the martensite inherited the ordered structure from the matrix, APBs being observed both in the martensite plates and the retained matrix. In the present study, APBs were observed only in the martensite plates, whereas the retained β was observed to contain only athermal or "diffuse" ω. The authors of this previous study [23] suggested a face centred orthorhombic unit cell with lattice parameters of $a = 0.457$ nm, $b = 0.490$ nm and $c = 0.299$ nm for the ordered martensite. However, this unit cell does not allow reflections of type $(0\,0\,1)\,\alpha''$, $(1\,1\,0)\,\alpha''$, and $(0\,2\,1)\,\alpha''$, etc., whereas these are allowed reflections for the unit cell proposed in the present study.

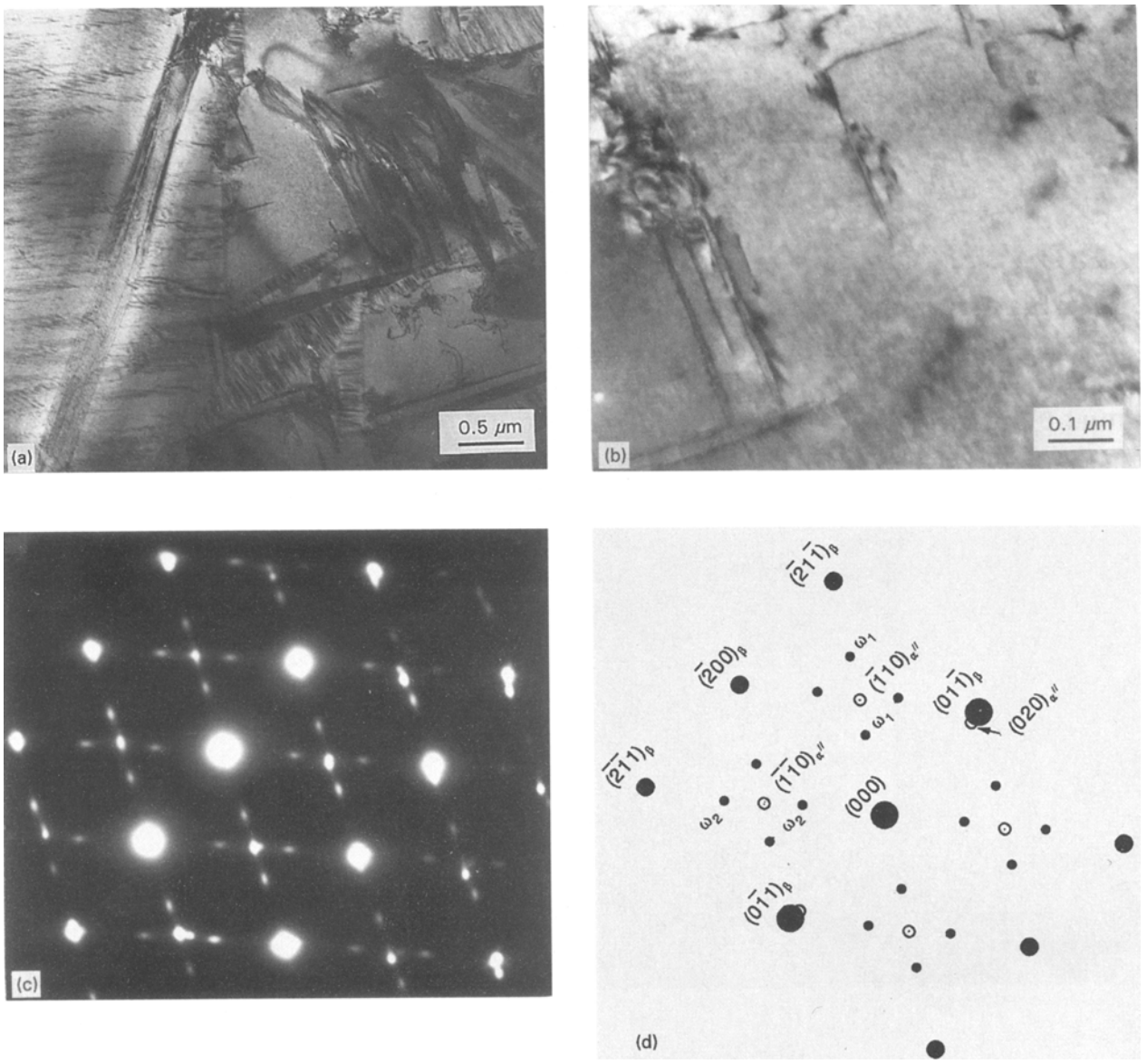

Figure 9 (a) Martensitic substructure in alloy Nb22L. (b) Fine athermal ω phase in the β matrix of alloy Nb22L. (c) SADP showing ω and α″ reflections, zone axes $[0\,1\,1]_{\beta}$ and $[0\,0\,1]_{\alpha''}$. (d) Index of the SADP shown in (c).

4.4. M_s Temperatures and effect of interstitials

Fig. 12 summarizes the effect of niobium on α′ and α″ martensite start temperatures, $M_{s\alpha'}$ and $M_{s\alpha''}$. Separate curves for α′ and α″ have been plotted following Flower *et al.* [24] with α′ being present in alloys containing Nb ≤ 7.2%. The proposed M_s curve places the upper compositional limit of α″ formation at approximately 23% Nb (Fig. 12 and Table III) in agreement with current results and those determined by Duwez [25], below Moffat and Larbalestiers' compositional limit of 25–29% Nb [3]. As discussed previously, the higher interstitial contents (especially oxygen) of Moffat and Larbalestiers' alloys is believed to have promoted the formation of α″ in the alloy containing 25% Nb, whereas the lower interstitial content used in the present work resulted in β + ω. This again reinforces the sensitivity of the M_s temperature to the interstitial content of the binary Ti–Nb alloys, a sensitivity also observed in this study, comparing the microstructures of Nb21H and Nb22L, Fig. 2a and c, the volume fraction of α″ martensite increased with increasing interstitial content. Finally, the volume fraction of α″ martensite in alloy Nb21H can be compared with that of a commercially produced alloy [15]. The interstitial content of Baker's alloy was not given, but the examination of his optical micrographs indicated a higher volume fraction of the α″ martensite than observed in Nb21H.

4.5. Ordering of martensite and effect of interstitials

Increased interstitial content not only promoted α″ formation, it also promoted the ordering of the orthorhombic martensite, with the order–disorder temperature being below the M_s temperature. For example, the higher interstitial content alloys Nb22H and Nb21H contained APBs within the martensite platelets, whereas an alloy with lower interstitial content,

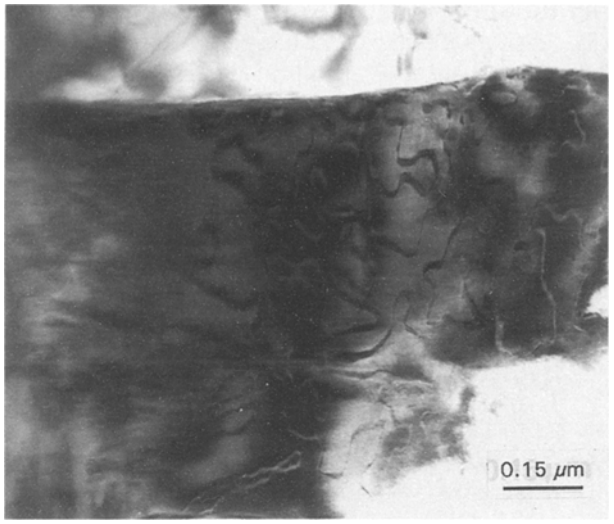

Figure 10 Bright-field-TEM image of alloy NB17 showing APBs in a martensite plate. The sample was prepared by ion milling.

TABLE III The phases present in alloys solution treated at 1000 °C and water quenched

Alloy	Actual Nb content (at %)	Total interstitial (w.p.p.m.)	Phases present
Nb17	17.6	830	$\alpha'' + \beta$
Nb18	18.2	550	$\alpha'' + \beta$
Nb19H	18.7	900	$\alpha'' + \beta$
Nb19L	19.4	500	$\alpha'' + \beta$
Nb20	19.6	440	$\alpha'' + \beta$
Nb21L	21.4	620	$\alpha'' + \beta + \omega$
Nb21H	21.4	1180	$\alpha'' + \beta + \omega$
Nb22H	21.7	1020	$\beta + \alpha'' + \omega$
Nb22L	21.9	450	$\beta + \alpha'' + \omega$[a]
Nb23	23.4	1170	$\beta + \alpha'' + \omega$
Nb24	24.1	660	$\beta + \omega$
Nb25	24.9	1080	β + diff ω
Nb26	25.6	940	β + diff ω

[a] No APBs were observed.

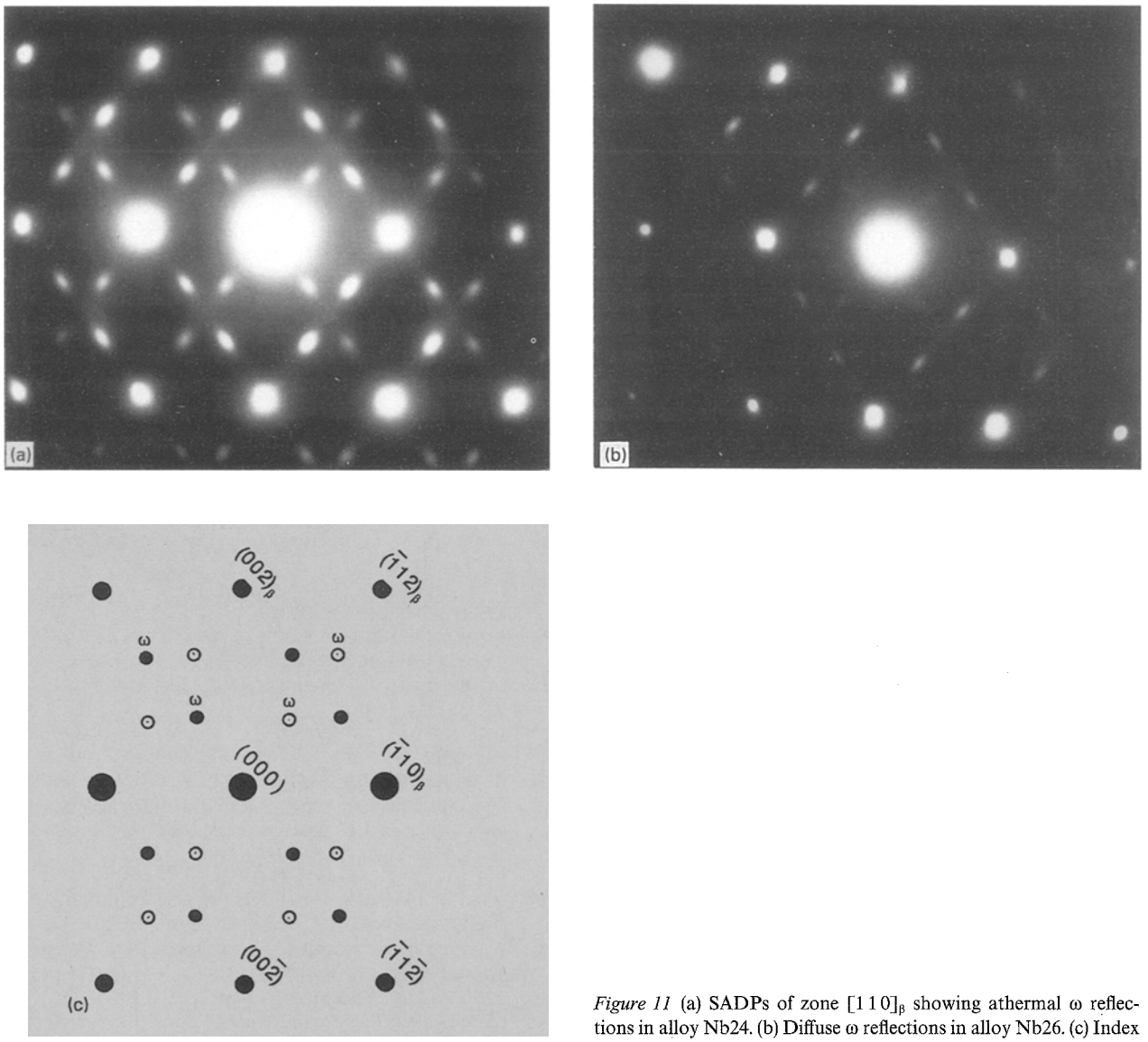

Figure 11 (a) SADPs of zone $[1\,1\,0]_\beta$ showing athermal ω reflections in alloy Nb24. (b) Diffuse ω reflections in alloy Nb26. (c) Index of the SADPs.

Nb22L, did not show evidence of ordering. Finally, Nb20, having a similar level of interstitial to Nb22L, went through the ordering reaction because lower niobium content raised the order–disorder temperature above room temperature. These effects of interstitial contents on the order–disorder and M_s temperatures are schematically illustrated in Fig. 13.

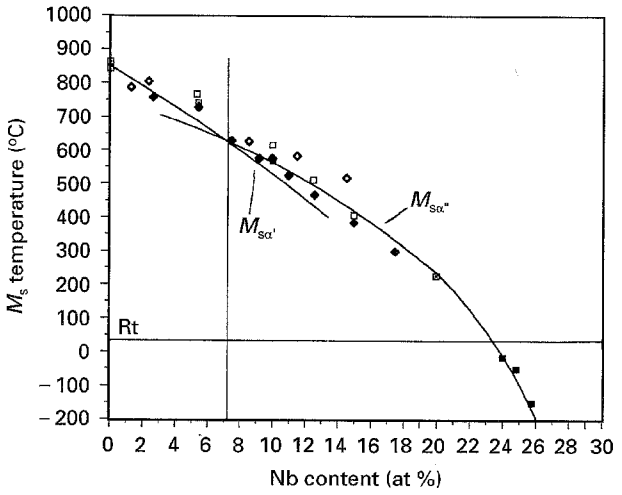

Figure 12 M_s curves for α′ and α″. (⊡) [6], (◆) [8], (□) [25], (◇) [26], (■) [27].

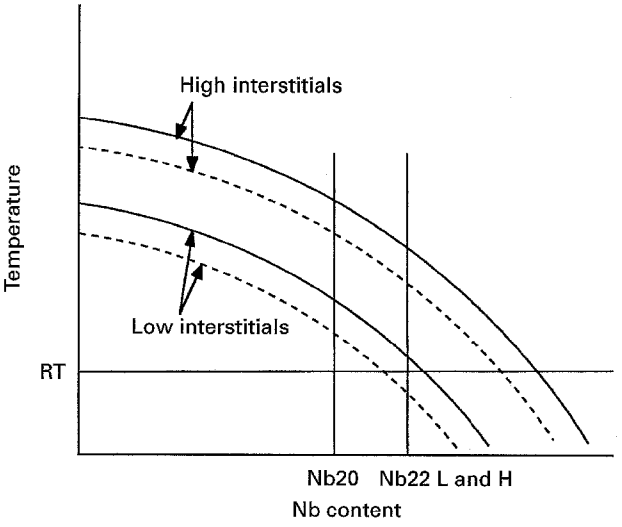

Figure 13 Schematic diagram showing the influence of interstitials on the (——) M_s and (– – –) order-disorder temperatures.

5. Conclusions

1. Alloys containing 16–23.4% Nb were transformed to an ordered base-centred orthorhombic martensite on quenching from the β-phase field.

2. The substructure of the martensite was generally composed of twins and stacking faults, the presence of APBs observed in the plates indicating that the martensite underwent ordering during quenching.

3. Both order–disorder and M_s temperatures were observed to be affected by the interstitial content, higher contents increasing both temperatures.

4. An increase in niobium content above 23.4% resulted in retention of the β-phase, containing either athermal ω or "diffuse" ω depending upon niobium and interstitial concentration.

5. The microhardness was observed to decrease with increase in niobium and decrease in interstitial contents.

Acknowledgements

The authors thank Osteonics, Inc. and Teledyne-Allvac for their sponsorship of this research project. The latter also provided the starting materials and performed the chemical analysis of the alloys.

References

1. J. L. MURRAY, "Phase Diagram of Binary Titanium Alloys" (ASM, Materials Park, OH, 1987) p. 188.
2. A. R. G. BROWN and K. S. JEPSON, *Mem. Sci. Rev. Metall.* **63** (1966) 575.
3. D. L. MOFFAT and D. C. LARBELIESTIER, *Metall. Trans.* **19** (1988) 1677.
4. Z. NISHIYAMA, "Martensitic Transformation" (Academic Press, New York, 1978) p. 67.
5. I. A. BAGARIATSKII, G. I. NOSOVA and T. V. TAGUNOVA, *Sov. Phys. Dokl.* **3** (1958) 1014.
6. A. R. G. BROWN, D. CLARK, J. EASTBROOK and K. S. JEPSON, *Nature* **201** (1964) 914.
7. B. A. HATT and V. G. RIVLIN, *Br. J. Appl. Phys.* **1** (1968) 1145.
8. K. S. JEPSON, A. R. G. BROWN and J. A. GRAY, "The Science Technology and Application of Titanium", edited by R. I. Jaffee and N. Promisel (Pergamon Press, London, 1970) p. 677.
9. J. P. MORNIROLI and M. GANTOIS, *Mem. Sci. Rev. Metall.* **70** (1973) 831.
10. A. T. BALCERZAK and S. L. SASS, *Metall. Trans.* **3** (1972) 1601.
11. O. LYON, *J. Less-Common Metals* **81** (1981) 103.
12. M. IKEDA, S. KOMATSU, T. SUGIMOTO and K. KAMEI, *J. Jpn. Inst. Metals* **52** (1988) 1206.
13. M. HANSON, E. L. KAMEN, H. D. KESSLER and D. J. McPHERSON, *Trans. AIME* **191** (1951) 881.
14. W. G. BRAMMER Jr and C. G. RHODES, *Philos. Mag.* **16** (1967) 477.
15. C. BAKER, *Metal Sci. J.* **5** (1971) 92.
16. M. G. MENDIRATTA, G. LUTGERING and S. WEISSMAN, *Metall. Trans.* **2** (1971) 2599.
17. B. OBST, D. PATTANAYAK and P. HOCHSTUHL, *J. Low-Temp. Phys.* **41** (1980) 595.
18. "Least Square Unit Cell Refinement", Program after Appleman and Evans (1973) implementation by R. G. Garvey, North Dakota State University, Fargo, ND, June 1984.
19. R. DAVIS, H. M. FLOWER and D. R. F. WEST, *J. Mater. Sci.* **14** (1979) 712.
20. D. L. MOFFAT, PhD thesis, University of Wisconsin-Madison, Madison, W (1985).
21. FU-WEN LING, H. J. RACK and E. A. STARKE Jr, *Metall. Trans.* **4** (1973) 1671.
22. FU-WEN LING, E. A. STARKE Jr. and B. G. LEFEVRE, *ibid.* **5** (1974) 179.
23. J. S. LEE PAK, C. Y. LEI and C. M. WAYMAN, *Mater. Sci. Eng.* **A132** (1991) 237.
24. H. M. FLOWER, R. DAVIS and D. R. F. WEST, in "Titanium and Titanium Alloys: Scientific and Technological Aspects", edited by J. C. Williams and A. F. Belov, Vol. 3 (Plenum Press, New York, 1982) p. 1703.
25. P. DUWEZ, *Trans. ASM* **45** (1953) 934.
26. H. KENEKO and Y. C. HUANG, *Nippon Kinzoku Gakki* **27** (1963) 387.
27. T. AHMED, M. LONG and H. J. RACK, Les Alliages de Titane Beta, eds A. Vassel, D. Eylon and Y. Combre. *De la Revue de Metallurgie* (Paris, France) (1995) 109–16. in "Proceedings of the International Workshop on β Titanium Alloys", Societe Francaise de Metallurgie et de Materiaux, Paris, (1994) in press.

Received 8 August
and accepted 21 December 1995